ACS APPLIED MATERIALS & INTERFACES

Research Article

www.acsami.org

Rapid Dye Adsorption via Surface Modification of TiO_2 Photoanodes for Dye-Sensitized Solar Cells

Boeun Kim,[†,‡] Se Woong Park,[†] Jae-Yup Kim,[†] Kicheon Yoo,[†] Jin Ah Lee,[†] Min-Woo Lee,[†] Doh-Kwon Lee,[†] Jin Young Kim,[†] BongSoo Kim,[†] Honggon Kim,[†] Sunghwan Han,[‡] Hae Jung Son,*[,†] and Min Jae Ko*[,†]

[†]Photo-Electronic Hybrids Research Center, Korea Institute of Science and Technology (KIST), Seoul 136-791, Republic of Korea

[‡]Department of Chemistry, Hanyang University, Wangsimni-ro 222, Seongdong-gu, Seoul 133-791, Republic of Korea

Supporting Information

ABSTRACT: A facile method for increasing the reaction rate of dye adsorption, which is the most time-consuming step in the production of dye-sensitized solar cells (DSSCs), was developed. Treatment of a TiO_2 photoanode with aqueous nitric acid solution (pH 1) remarkably reduced the reaction time required to anchor a carboxylate anion of the dye onto the TiO_2 nanoparticle surface. After optimization of the reaction conditions, the dye adsorption process became 18 times faster than that of the conventional adsorption method. We studied the influence of the nitric acid treatment on the properties of TiO_2 nanostructures, binding modes of the dye, and adsorption kinetics, and found that the reaction rate improved via the synergistic effects of the following: (1) electrostatic attraction between the positively charged TiO_2 surface and ruthenium anion increases the collision frequency between the adsorbent and the anchoring group of the dye; (2) the weak anchoring affinity of NO_3^- in nitric acid with metal oxides enables the rapid coordination of an anionic dye with the metal oxide; and (3) sufficient acidity of the nitric acid solution effectively increases the positive charge density on the TiO_2 surface without degrading or transforming the TiO_2 nanostructure. These results demonstrate the developed method is effective for reducing the overall fabrication time without sacrificing the performance and long-term stability of DSSCs.

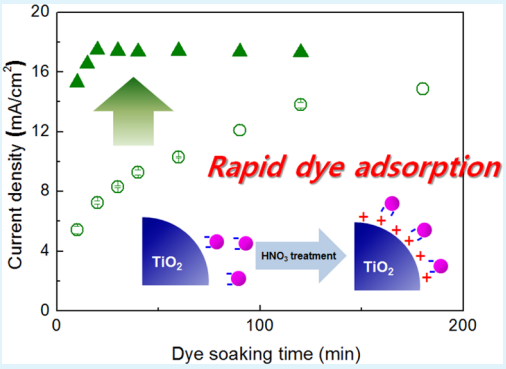

KEYWORDS: *dye-sensitized solar cells, dye adsorption, reaction kinetics, acid treatment, adsorption time*

INTRODUCTION

Dye-sensitized solar cells (DSSCs) have attracted great attention from the academia and the industry because of their cost-effectiveness, ease of device fabrication, and nontoxic materials. To date, record-setting efficiencies of ~11−12% for small cells and ~9.9% for modules have been reported.[1−4] Excellent device stability has been shown in both the accelerated aging tests and outdoor testing. For example, Desilvestro and a co-workers reported a device showing only 17% efficiency loss after continuous radiation of one sun light at 55 °C for 25 000 h.[5] In addition, DSSC research has made important contributions to the development of the core regions of photoelectrochemistry and material science.[6,7] However, for DSSC technology to achieve the goal of providing electricity at a competitive price below $1.0/Watt peak (more preferably at $0.50/Watt peak) and therefore, become established as the cheapest candidate for future energy production, the solar cell efficiency should be further enhanced and cost-effective manufacturing processes with high productivity are required.

DSSCs are typically prepared through several processing steps: assembly of a dye adsorbed TiO_2 photoanode onto transparent conductive oxide (TCO) and a Pt-coated TCO cathode followed by filling the space between the two electrodes with redox electrolyte.[8,9] Among these steps, the adsorption of dye molecules onto the TiO_2 nanoparticle surfaces is very important for achieving high DSSC power conversion efficiencies (PCEs) and productivity. To attach the dye molecules to the surface, anchoring groups that form linkages to the metal oxide are incorporated into the dye sensitizers.[1] The most common anchoring group is carboxylic acid (−COOH), which can coordinate to the metal core in unidentate, chelating, and bridging bidentate modes. The dye adsorption mechanism is composed of three consecutive steps: (1) mass transfer, i.e., external diffusion of the dye molecules to the outer surfaces of the TiO_2 nanoparticles; (2) internal diffusion, i.e., diffusion of the dye molecules into the pores of the TiO_2 nanoparticles; and (3) chemical reaction, i.e., chemisorption, which involves the coordination of a carboxylate ion in the dye to the titanium atom.[10−12] Dye adsorption is the most time-consuming step of DSSC fabrication. Therefore,

Received: March 21, 2013
Accepted: May 6, 2013
Published: May 16, 2013

reducing the time required for dye adsorption would significantly reduce the overall fabrication time. Accordingly, it is necessary to develop an easy and efficient processing method that reduces the time required for dye adsorption and achieves high PCEs. A wide range of research has been conducted to improve the dye adsorption process by modifying the metal oxide surface.[13−15] For example, an electric field or ultrasonication were applied to the metal oxide surface; however, these methods are not suitable for large-scale commercial DSSCs. Meanwhile, in order to provide functional groups on the metal surface that can efficiently coordinate with carboxylates, the metal oxide surface is treated with acids such as sulfuric acid, acetic acid, and nitric acid leading to enhanced solar cell performance. It has been reported that ionization of metal oxide via acid treatment remarkably enhances the interactions of the metals with the dye sensitizers.[16−18] Inspired by these results, we developed a method to increase the reaction rate for dye adsorption by modifying the charge density on the surface of the TiO_2 nanoparticles.

Herein, we introduce a facile method of anchoring a ruthenium dye sensitizer onto the surface of TiO_2, and discuss the effects of acid treatment on dye adsorption. The developed method results in much more rapid metal coordination. Thus, the dye adsorption process becomes 18 times faster after the optimization of adsorption temperature and dye concentration.

RESULTS AND DISCUSSION

Effects of Reaction Temperature and Dye Concentration on Dye Adsorption. Because adsorption depends on reaction conditions such as temperature and reactant concentration, we optimized the conditions for high photocurrent density by testing a series of DSSCs obtained considering dye adsorption temperatures and dye concentrations. Temperature has an important effect on the adsorption process because the adsorption is endothermic[20] and the diffusion rate of adsorbate molecules across the internal pores in the adsorbent particles increases at a higher temperature.[21] Taking these into consideration, we increased the dye adsorption temperature a little bit from room temperature to 40 °C, which could be applicable for the mass-production. To estimate the number of dye molecules adsorbed onto the TiO_2 nanoparticle, we measured the short-circuit current density (J_{sc}) of the DSSCs because J_{sc} is normally proportional to the total amount of adsorbed dye. Figure 1 shows that J_{sc} linearly increased close to 17 mA/cm^2 when the reaction time was extended from 0 to 2 h. In contrast, the DSSCs that underwent dye adsorption at room temperature needed a much longer reaction time to achieve similar J_{sc} values. For example, at room temperature, 6 h of immersion was required to achieve a J_{sc} of above 16.5 mA/cm^2. It is notable that both the DSSCs show similar J_{sc} performances if the reaction time is sufficient for dye adsorption, suggesting that the total number of the dye molecules adsorbed at a saturation point is not dependent on the reaction temperature. Using a concentrated dye solution also reduces the reaction time and improves the DSSC performance.[22] Thus, we attempted to optimize the concentration of the dye solution by measuring the J_{sc} values of DSSCs prepared using different dye concentrations. The TiO_2 photoanodes were dipped into dye solutions with concentrations varying from 0.5 to 5 mM for 10 min at 40 °C. After rinsing the dye-coated electrode with ethanol, it was used as the photoanode of a DSSC for photovoltaic measurement. As shown in Figure 2, J_{sc} linearly increased with increasing concentration from 0.5 to 2.0 mM. On the basis of these results, we determined the reaction time required for DSSCs to have the highest J_{sc} value when fabricated using a 2 mM dye solution at 40 °C. In comparison with the DSSC fabricated using a conventional 0.5 mL dye solution, the reaction time required to reach a saturation point is significantly reduced, i.e., from 2 h to 40 min. As a result, by controlling the reaction temperature and dye concentration, we efficiently reduced the overall processing time for dye adsorption from 6 h to 40 min.

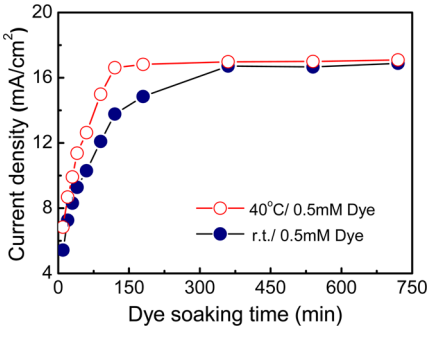

Figure 1. Short-circuit current densities of DSSCs measured as a function of dye soaking time at room temperature (blue) and 40 °C (red). All values were averaged from the results for three DSSCs.

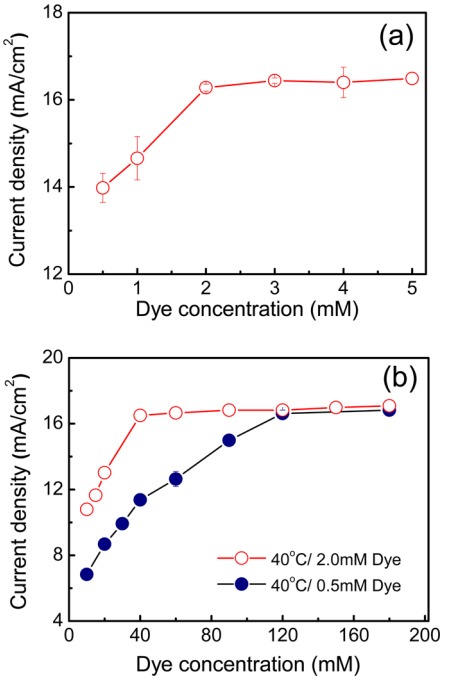

Figure 2. Short-circuit current densities of DSSCs with respect to (a) dye concentration and (b) dye soaking time using dye solutions of 0.5 (blue) and 2 mM (red) at 40 °C. All values were averaged from the results for three DSSCs.

Effects of Acid Treatment of TiO_2 Particles on Dye Adsorption. Using the optimized reaction temperature and dye concentration, we investigated the effects of acid treatment of a TiO_2 photoanode on dye adsorption. Nitric acid was chosen because NO_3^- anchors more weakly to TiO_2 than other acids such as acetic acid and phosphoric acid; therefore, it is

more readily replaced by a carboxylate ion of the dye. It is reported that carboxylate and phosphate ions form strong bonds with the titanium atom of the TiO_2 nanoparticle. This prevents efficient dye adsorption, resulting in decreased amounts of the adsorbed dyes and low incident photon-to-current efficiencies (IPCEs).[18,23] The TiO_2 films were immersed into nitric acid solutions with acidity ranging from pH 1 to 5 and then dipped into a 2 mM dye solution for 5 min at 40 °C. The lowest acidity used in the experiment is pH 1 because too low acidity can destroy the anatase of the TiO_2 nanoparticles.[24] The photovoltaic performances of the DSSCs were tested and the results are shown in Figure 3. The J_{sc} value

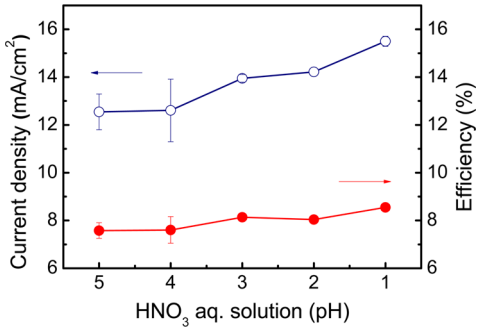

Figure 3. Short-circuit current densities (blue) and power conversion efficiencies (red) of DSSCs as a function of the acidity of a nitric acid solution. All values were averaged from the results for four DSSCs.

gradually increased from 12.5 mA/cm^2 at pH 5 to 15.5 mA/cm^2 at pH 1, while the PCE increased to 8.6%. When the electrode dipping time was extended to more than 20 min, the DSSCs achieved PCEs of >9% with J_{sc} values being more than 17 mA/cm^2, although the fill factor (FF) slightly decreased. We did not find any significant change in V_{oc}s after the nitric acid treatment although it was reported that the acid treatment of TiO_2 photoelectrodes could cause reduction of V_{oc} values by inducing positive shifts in the conduction band of TiO_2 photoelectrodes.[25,26] Some of other research groups also reported similar results to our observations.[18,24] They found that charge recombination from electrons in TiO_2 conduction bands to I_3^- in electrolyte was suppressed after acid treatment. As a result, the V_{oc} loss due to positive shifts of the flat band potential of TiO_2 might be compensated by this V_{oc} gain. Regarding this issue, detailed studies are in progress. All solar cell parameters measured as a function of the adsorption time are recorded in Table 1.

It is interesting that, as shown in Figure 4, the DSSCs prepared without nitric acid treatment achieved very similar J_{sc}

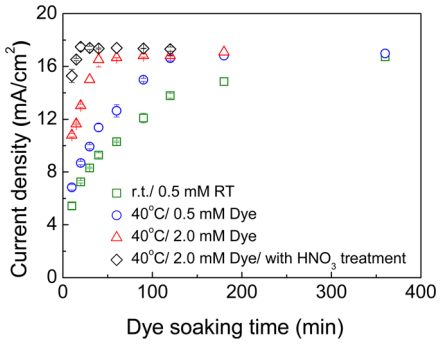

Figure 4. Comparisons of short-circuit current densities among DSSCs prepared using various dye adsorption conditions. All values were averaged from the results for three DSSCs.

values if the dipping time for dye adsorption was extended sufficiently. For example, the DSSC fabricated using a 0.5 mM dye solution at room temperature without nitric acid treatment eventually reached a J_{sc} value close to 17 mA/cm^2 although the processing time required is 18 times longer than that for the DSSC prepared with the nitric acid treatment. This result indicates that the main effect of the acid treatment is increasing the reaction rate for dye adsorption onto the TiO_2 nanoparticle rather than improving the photocurrent of the DSSC by increasing the amount of the adsorbed dye.

To further elucidate the effect of the nitric acid treatment and its mechanism, we conducted a series of experiments. The morphology of the TiO_2 nanoparticle was characterized using field emission scanning electron microscopy (FE-SEM). Images a and b in Figure S1 in the Supporting Information show the images of the nitric acid-treated and -untreated TiO_2 nanoparticles. No obvious difference is observed in the topological features, which suggests that nitric acid does not induce any significant morphological change in the TiO_2 nanoporous structure. The microstructure of the TiO_2 photoanode is also expected to be unchanged with the nitric acid treatment. From electrochemical impedance spectroscopy in Figure S2 in the Supporting Information, the shape of Nyquist plot in the impedance spectrum of the DSSC with the nitric acid treatment is very similar to that of the DSSC without the treatment, implying that the microscopic structure of TiO_2 is almost conserved after the nitric acid treatment. This is in contrast to the result reported by Watson et al., in which the nitric acid treatment led to significant changes in the

Table 1. Photovoltaic Parameters of DSSCs Containing TiO_2 Photoanodes Treated with pH 1 Nitric Acid Solution[a]

adsorption time (min)	J_{sc} (mA/cm^2)	V_{oc} (mV)	FF (%)	PCE (%)
5	13.60 ± 0.30	787.2 ± 3.5	70.76 ± 0.46	7.57 ± 0.21
10	15.28 ± 0.19	776.5 ± 4.1	68.54 ± 0.53	8.13 ± 0.20
15	16.52 ± 0.23	782.2 ± 4.0	68.04 ± 0.50	8.80 ± 0.01
20	17.48 ± 0.29	781.9 ± 1.4	67.29 ± 0.12	9.20 ± 0.12
30	17.40 ± 0.13	784.7 ± 5.2	67.59 ± 0.30	9.23 ± 0.04
40	17.37 ± 0.11	789.9 ± 3.2	67.11 ± 0.13	9.21 ± 0.02
60	17.40 ± 0.12	782.2 ± 1.7	66.77 ± 0.30	9.09 ± 0.03
90	17.36 ± 0.02	782.8 ± 0.8	66.93 ± 0.06	9.09 ± 0.01
120	17.31 ± 0.16	781.7 ± 2.1	66.99 ± 0.72	9.06 ± 0.04

[a]All values were averaged from the results from three DSSCs.

dx.doi.org/10.1021/am401034r | ACS Appl. Mater. Interfaces 2013, 5, 5201−5207

microstructures of the top surface of the electrode and alternation in the pore size of the TiO_2.[27] These different results may be due to the different concentrations of nitric acid solutions used: we carried out with a 0.1 M (pH 1) nitric acid solution, whereas Watson et al. performed with that of 2 M, which is 20 times more concentrated than ours.

To gain a deeper insight into the TiO_2 nanostructure at a molecular level, wer performed Raman and attenuated total reflectance Fourier transform infrared (ATR-FTIR) spectroscopy studies. As shown in Figure S3 in the Supporting Information, the Raman spectra of the nitric acid-treated and -untreated TiO_2 nanoparticles showed the normal modes of anatase at 143, 397, 517, and 637 cm^{-1}, assigned to the E_g, B_{1g}, A_{1g}, and B_{2g} modes, respectively.[11] The intensity of these key features was almost conserved and no new peak appeared after the acid treatment. The binding mode of the carboxylate in the Ru dye with TiO_2 contributes to the understanding of the nanostructure of the dye adsorbed TiO_2 nanoparticle. In the ATR-FTIR spectra (see Figure S4 in the Supporting Information), the peaks at 1600 and 1377 cm^{-1} are assigned to the ν(COO- asym) and ν(COO- sym) carboxylate vibrations,[11] respectively, and were almost equivalent after nitric acid treatment. From this result, it is evident that nitric acid treatment does not significantly affect the nanostructure or the binding mode of TiO_2 with carboxylates of the dye.

We compared the total amount of the adsorbed dye on the TiO_2 surface of DSSCs prepared via treatment with nitric acid solutions having pH values of 1−3. The numbers of adsorbed dye molecules for each cell were determined by dissolving the anchored dye into 100 mL NaOH solution and then measuring the UV−vis spectra of the dye solution. When the dye-adsorption time was limited to 10 min (Table 2), the amount of dye that desorbs from the TiO_2 surface increases as the acidity decreases from that of deionized water (7.13×10^{-8} mol/cm^2) to that of a pH 1 nitric acid solution (9.21×10^{-8} mol/cm^2); however, with 1800 min of adsorption time and a dye concentration of 0.5 mM, the amount of the desorbed dye from the nitric acid-treated (pH 1) and -untreated cells was similar. This indicates that the total number of dye molecules at an equilibrium is not influenced by the nitric acid treatment. In addition, we monitored the adsorption amount at 20, 30, 40, and 50 °C using 2.0 mM dye solutions. When TiO_2 was treated with a nitric acid solution (pH 1), the concentration of the dissolved dye molecules reached 6.30×10^{-8} mol/cm^2 at a saturation point, although the time required to reach this point varied (Figure 5); at higher temperatures, the saturation occurred in a shorter time. Without nitric acid treatment, the adsorption was much slower; after 90 min, only the systems that were heated at 50 °C reached the saturation point.

Table 2. Amounts of Dye Adsorbed under Various Conditions

treatment solution	concentration (mM)	adsorption time (min)	amount of dye[a] (mol/cm^2)
HNO_3 aq. (pH 1)	2.0	10	9.21×10^{-8}
HNO_3 aq. (pH 2)	2.0	10	8.28×10^{-8}
HNO_3 aq. (pH 3)	2.0	10	7.52×10^{-8}
none	2.0	10	7.13×10^{-8}
DI water	2.0	10	6.98×10^{-8}
none	0.1	1800	9.46×10^{-8}
none	0.5	1800	1.05×10^{-7}
none	2.0	1800	1.06×10^{-7}
HNO_3 aq. (pH 1)	2.0	1800	1.09×10^{-7}

[a]Amount of adsorbed dye molecules were calculated by dissolving the anchored dye into 100 mL NaOH solution and measuring the relative absorption peak intensity at 530 nm in the UV−vis spectra of the resultant solution.

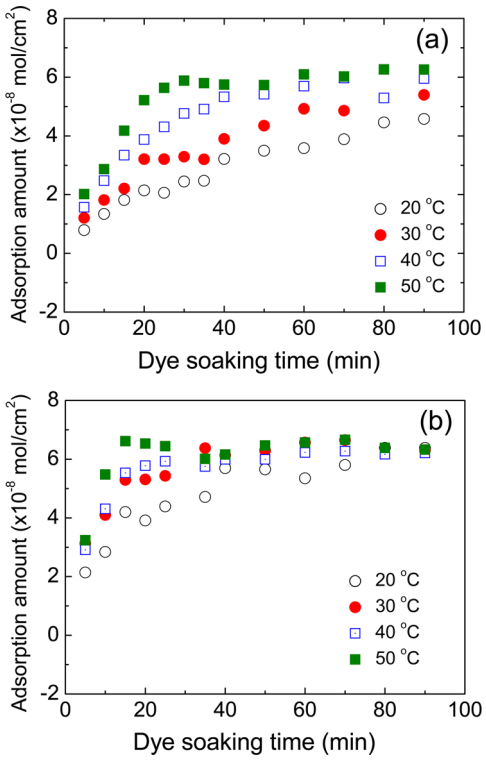

Figure 5. Amounts of N719 dye adsorbed on DSSCs prepared (a) without nitric acid treatment and (b) with nitric acid treatment as a function of soaking time at various temperatures. The TiO_2 film thickness is ~7 μm.

On the basis of the experimental data, we conclude that nitric acid treatment of TiO_2 nanoparticles enhances the speed of dye adsorption but does not significantly influence the overall properties of the dye-adsorbed TiO_2 nanoparticles such as nanoporous structure, dye anchoring mode, and the amount of adsorbed dye at an equilibrium. The next stage of our research is the study of the kinetics of dye adsorption onto TiO_2 nanoparticles and the adsorption mechanism.

Kinetics of Dye Adsorption onto TiO_2 Nanoparticles. Adsorption kinetics can be used to estimate the rate of dye adsorption onto TiO_2 nanoparticles and provide an adsorption mechanism. We denote the dye adsorbed TiO_2 as TiO_2:dye; the reaction can be represented as follows

$$\text{dye} + TiO_2 \rightarrow TiO_2\text{: dye} \quad (1)$$

The reaction rate (r) can be expressed similar to that of a common concentration-dependent chemical reaction according to a previous research result.[22] Therefore, if it is assumed that the concentration of the dye is constant and the total number of binding sites in the TiO_2 nanoparticle is the same as the total number of dye molecules at a saturation point, the following pseudoreaction equation is obtained

$$r = d[\mathrm{TiO_2}\text{: dye}]_t/dt = -d([\mathrm{TiO_2}\text{: dye}]_{sat} - [\mathrm{TiO_2}\text{: dye}]_t)/dt = k[\mathrm{TiO_2}]^n[\mathrm{dye}]^m = k'[\mathrm{TiO_2}]^n = k'([\mathrm{TiO_2}\text{: dye}]_{sat} - [\mathrm{TiO_2}\text{: dye}]_t)^n \quad (2)$$

where k and k' are the reaction rate constant and $k[\mathrm{dye}]^m$, respectively. n and m represent reaction orders. $[\mathrm{TiO_2}]$ indicates the concentration of adsorption sites in the TiO_2 nanoparticle, which can be represented as $([\mathrm{TiO_2}\text{:dye}]_{sat} - [\mathrm{TiO_2}\text{:dye}]_t)$ in which $[\mathrm{TiO_2}\text{:dye}]_{sat}$ and $[\mathrm{TiO_2}\text{:dye}]_t$ are the amounts of the dye adsorbed at the saturation point and time t, respectively. If the reaction is assumed to be first order, as demonstrated in the previous result,[22] eq 2 can be expressed as eq 3 using θ, which represent the portion of dye adsorbed after a specific soaking time (t) and is defined as $[\mathrm{TiO_2}\text{:dye}]_t/[\mathrm{TiO_2}\text{:dye}]_{sat}$.

$$r = -d(1-\theta)/dt = k'(1-\theta) \quad (3)$$

From eq 3, we can obtain the next equation

$$\ln(1-\theta) = -k't \quad (4)$$

The saturated concentration ($[\mathrm{TiO_2}\text{:dye}]_{sat}$) occurs when $d[\mathrm{TiO_2}\text{:dye}]_t/dt$ becomes close to zero. Because the equation is known to be pseudofirst-order, k' can be calculated by plotting the soaking time versus $\ln(1-\theta)$, as shown in Figure 6. The dye coverage (θ) was calculated from the results shown in Figure 5 according to the method reported previously.[22] For both the nitric acid-treated and -untreated DSSCs, the $\ln(1-\theta)$ values were in inverse proportion to the dye adsorption time, indicating that our data was first order. We calculated the k' values at four different temperatures and determined that the k' value of the nitric acid-treated cell is ~2−3 times higher than that of the corresponding untreated cell.

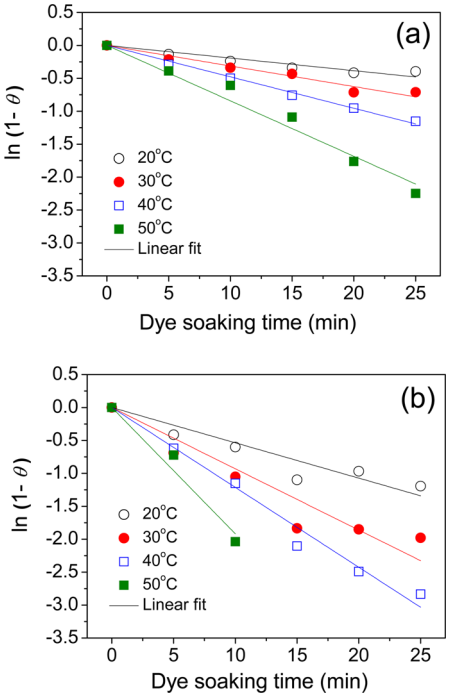

Figure 6. Dye coverage versus soaking time for DSSCs (a) without nitric acid treatment and (b) with nitric acid treatment based on pseudofirst-order reaction showing a linear relationship between $\ln(1-\theta)$ and the soaking time.

We calculated the activation energy for dye adsorption onto the TiO_2 nanoparticle using the Arrhenius equation as follows[28]

$$\ln k = \ln A - E_a/\mathrm{RT} \quad (5)$$

where k is the reaction rate constant ($k = k'/[\mathrm{dye}]^m$) obtained from the pseudofirst-order kinetic model, R is the universal gas constant (8.314 $JK^{-1}mol^{-1}$), A represents a pre-exponential factor, and E_a is calculated as the negative value of the logarithm of the k values with respect to the inverse of the absolute temperature (T). Therefore, eq 5 can be expressed as eq 6.

$$\ln k' = \ln A - E_a/\mathrm{RT} + m\ln[\mathrm{dye}] \quad (6)$$

When $\ln k'$ is plotted against $1/T$, a straight line with a slope of E_a/R is obtained (Figure 7). Both the DSSCs showed very similar activation energies: the activation energies of the nitric acid-treated and -untreated cells were 3.7×10^4 and 3.2×10^4 J mol^{-1}, respectively. However, A of the nitric acid-treated DSSC was three times greater than that of the untreated cell; A is mostly dependent on the collision frequency between reactants, which illustrates how frequently collision occurs between carboxylates and the binding sites in TiO_2 nanoparticles.[28]

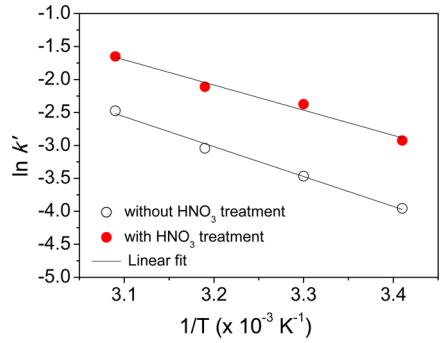

Figure 7. Arrhenius plots of logarithm of k' versus the inverse of absolute temperature.

Because the activation energies for dye adsorption and dye binding modes are very similar for the nitric acid-treated and -untreated TiO_2 nanoparticles, nitric acid treatment is not considered to influence the mechanism of the chemical reaction between the carboxylate of the dye and the TiO_2 nanoparticle; therefore, the chemical reaction is not the source of the difference in the reaction rate. Electrostatic interactions can be significantly involved because the charge density on metal oxide surfaces is affected by acid treatment and increases when treated with an acid solution of higher acidity.[29,30] From zeta potential measurements, it was determined that the surface charge of the acid-treated TiO_2 nanoparticles (+32.18 mV) is much higher than that of the untreated TiO_2 nanoparticles (+9.36 mV). Because the reactive dye has anionic character because of the carboxylate moiety, electrostatic attraction between the dye and the TiO_2 surface may increase significantly after nitric acid treatment, leading to more frequent collisions between the carboxylates and the reactive sites on the TiO_2 surface. Decreasing the pH value of the nitric acid solution increases the number of positively charged sites on the TiO_2 nanoparticle according to eqs 7 and 8, thus resulting in increased favorable interactions of the TiO_2 surface with the dye anion because of electrostatic attraction.[31] This is supported by the research work reported by Sharma et al.,[32] where electrostatic attractions between a positively charged

TiO_2 photoanode and a negatively charged end of a dye molecule led to increase of dye adsorption and as a result, a photocurrent density of a DSSC was enhanced.

$$Ti^{4+} - OH + H^+ \leftrightarrow Ti^{4+} - OH_2^+ \quad (7)$$

$$Ti^{4+} - O - Ti^{4+} + H^+ \leftrightarrow Ti^{4+} - OH^+ - Ti^{4+} \quad (8)$$

In summary, nitric acid treatment of the TiO_2 photoanode remarkably reduced the reaction time required for dye adsorption; this can be explained via several synergistic effects: first, the enhanced electrostatic attraction of the anchoring group of the Ru dye with the TiO_2 nanoparticle increases the collision frequency. Second, the weak anchoring affinity of NO_3^- with TiO_2 enabled a fast chemisorption reaction between carboxylate and TiO_2. Finally, proper acidity of the nitric acid solution effectively increased the positive charge on the TiO_2 surface without significantly affecting the TiO_2 nanostructure.

Influence of Nitric Acid Treatment on the Stability of DSSCs. To investigate the possibility of cell degradation caused by nitric acid treatment of the TiO_2 photoanode, we studied the long-term stability of the resultant DSSCs. The DSSCs were prepared from TiO_2 photoanodes treated with a nitric acid solution (pH 1) for 350 min and then immersed in a 0.5 mM N719 dye solution at room temperature. The characteristic photovoltaic parameters of the DSSCs were monitored for 30 days after storing the cells in the dark in 100% acetonitrile. As shown in Figure S5 in the Supporting Information, the PCE did not decrease significantly over the 30 days and the photovoltaic performance was comparable to that of the DSSC prepared without nitric acid treatment; this shows that the nitric acid treatment did not have a detrimental effect on the solar cell stability.

CONCLUSIONS

The time required for dye adsorption onto the TiO_2 photoanode was significantly reduced simply by treating the photoanode with a nitric acid solution. The nitric acid treatment effectively increased the collision frequency of carboxylates of the ruthenium dye with adsorption sites on the TiO_2 nanoparticle; thus, the reaction rate for dye adsorption was significantly improved. Nitric acid-treated and -untreated DSSCs showed comparable photovoltaic performance and long-term stability. The results show that the positively charged TiO_2 surface formed by nitric acid treatment induces high electrostatic attraction between the reaction sites and anionic dyes, resulting in a much faster adsorption reaction. Therefore, the overall processing time required for dye adsorption decreased from 6 h to 20 min using the optimized dye concentration and temperature for dye adsorption. We believe that the method developed for rapid dye adsorption enables an easier DSSC fabrication process and will considerably contribute to widespread use of DSSCs at a lower cost.

ASSOCIATED CONTENT

Supporting Information

Preparation of the TiO_2 photoanode, DSSC fabrication, FE-TEM characterization, Raman and ATR-FTIR spectroscopy of the TiO_2 nanoparticle, and photocurrent–voltage (J–V) measurements of the DSSCs. This material is available free of charge via the Internet at http://pubs.acs.org.

AUTHOR INFORMATION

Corresponding Author

*E-mail: mjko@kist.re.kr (M.J.K.); hjson@kist.re.kr (H.J.S.).

Notes

The authors declare no competing financial interest.

ACKNOWLEDGMENTS

This work was supported by the Global Frontier R&D Program on Center for Multiscale Energy System (2012M3A6A7054856), the Pioneer Research Program (2012-0005955) funded by the National Research Foundation (NRF) under the Ministry of Science, ICT & Future Planning (MSIP), Korea. The work was also supported by a grant from the New & Renewable Energy Program (2010T100100654, 2010T100100651) of the Korea Institute of Energy Technology Evaluation and Planning (KETEP) funded by the Ministry of Trade, Industry & Energy (MOTIE) and a grant from the KIST internal project (2E23821).

REFERENCES

(1) Hagfeldt, A.; Boschloo, G.; Sun, L.; Kloo, L.; Pettersson, H. *Chem. Rev.* **2010**, *110*, 6595–6663.
(2) Yella, A.; Lee, H.-W.; Tsao, H. N.; Yi, C.; Chandiran, A. K.; Nazeeruddin, M.; Diau, E. W.-G.; Yeh, C. Y.; Zakeeruddin, S. M.; Grätzel, M. *Science* **2011**, *334*, 629–634.
(3) Green, M. A.; Emery, K.; Hishikawa, Y.; Warta, W. *Prog. Photovoltaics* **2011**, *19*, 84–92.
(4) McGehee, M. D. *Science* **2011**, *334*, 607–608.
(5) Harikisun, R.; Desilvestro, H. *Sol. Energy* **2011**, *85*, 1179–1188.
(6) Memming, R. *Semiconductor Electrochemistry*; Wiley–VCH: Weinheim, Germany, 2001.
(7) Würfel, P. *Physics of Solar Cells: From Principles to New Concepts*; Wiley–VCH: Weinheim, Germany, 2005.
(8) Pettersson, H.; Gruszecki, T.; Johansson, L.-H.; Johander, P. *Sol. Energy Mater. Sol. Cells* **2003**, *77*, 405–413.
(9) I, S.; Murakami, T.; Comte, P.; Liska, P.; Gr€atzel, C.; Nazeeruddin, M. K.; Grätzel, M. *Thin Solid Films* **2008**, *516*, 4613–4619.
(10) Galoppini, E. *Coord. Chem. Rev.* **2004**, *248*, 1283–1297.
(11) Lee, K. E.; Gomez, M. A.; Elouatik, S.; Demopoulos, G. P. *Langmuir* **2010**, *26*, 9575–9583.
(12) Leon, C. P.; Kador, L.; Peng, B.; Thelakkat, M. *J. Phys. Chem. B* **2006**, *110*, 8723–8730.
(13) Nazeeruddin, M. K.; Splivallo, R.; Liska, P.; Comte, P.; Grätzel, M. *Chem. Commun.* **2003**, *12*, 1456–1457.
(14) Seo, Y.; Kim, J. H. *J. Ind. Eng. Chem.* **2013**, *19*, 488–492.
(15) Seo, H.; Son, M.-K.; Shin, I.; Lee, J.-K.; Prabakar, K.; Kim, H.-J. *Electrochim. Acta* **2010**, *55*, 4120–4123.
(16) Hirose, F.; Kuribayashi, K.; Suzuki, T.; Narita, Y.; Kimura, Y.; Niwano, M. *Electrochem. Solid-State Lett.* **2008**, *11*, A109–A111.
(17) Hao, S.; Wu, J.; Fan, L.; Huang, Y.; Lin, J.; Wei, Y. *Sol. Energy* **2004**, *76*, 745–750.
(18) Wang, Z.-S.; Yamaguchi, T.; Sugihara, H.; Arakawa, H. *Langmuir* **2005**, *21*, 4272–4276.
(19) Pettibone, J. M.; Cwiertny, D. M.; Scherer, M.; Grassian, V. H. *Langmuir* **2008**, *24*, 6659–6667.
(20) Hwang, K.-J.; Im, C.; Cho, D. W.; Yoo, S.-J.; Lee, J.-W.; Shim, W.-G. *RSC Adv.* **2012**, *2*, 3034–3048.
(21) Hirose, F.; Shikaku, M.; Kimura, Y.; Niwano, M. *J. Electrochem. Soc.* **2010**, *157*, B1578–B158.
(22) Lee, C. R.; Kim, H.-S.; Jang, I.-H.; Im, J.-H.; Park, N.-G. *ACS Appl. Mater. Interfaces* **2011**, *3*, 1953–1957.
(23) Jung, H. S.; Lee, J.-K.; Lee, S.; Hong, K. S.; Shin, H. *J. Phys. Chem. C.* **2008**, *112*, 8476–8480.
(24) Jung, H. S.; Shin, H.; Kim, J.-R.; Kim, J. Y.; Hong, K. S. *Langmuir* **2004**, *20*, 11732–11737.

(25) Redmond, G.; Fitxmaurice, D. *J. Phys. Chem.* **1993**, *97*, 1426−1430.
(26) O'Regan, B.; Grätzel, M.; Fitzmaurice, D. *Chem. Phys. Lett.* **1991**, *183*, 89−93.
(27) Watson, T.; Charbonneau, C.; Bryant, D.; Worsley, D. *Int. J. Photoenergy* **2012**, 8.
(28) Ball, D. W. In *Physical Chemistry*; Brooks/Cole Publishing: Pacific Grove, CA, 2002.
(29) Belessi, V.; Romanos, G.; Boukos, N.; Lambropoulou, D.; Trapalis, C. *J. Hazard. Mater.* **2009**, *170*, 836−844.
(30) Qu, P.; Meyer, G. J. *Langmuir* **2001**, *17*, 6720−6728.
(31) Connor, P. A.; Dobson, K. D.; McQuillan, A. J. *Langmuir* **1999**, *15*, 2402−2408.
(32) Balraju, P.; Kumar, M.; Roy, M. S.; Sharma, G. D. *Synth. Met.* **2009**, *159*, 1325−1331.